

Common sense and Semantically Grounded Understanding for Effective Room Navigation in Embodied Environment

Abstract

1 Previous multi-modal embodied navigation research focused
2 on completing tasks by aligning image features with natural
3 language instructions. In this paper, we investigate if intrinsic
4 features such as common sense and semantic understanding,
5 which are critical for human navigators but ignored in pre-
6 vious research, also help artificial agents navigate in realis-
7 tic 3D environments given a high-level linguistic instruction.
8 From our experiments, we observe that common sense helps
9 the agent in long-term planning, while semantic understand-
10 ing helps the agent in local planning in the room navigation
11 (*RoomNav*) task. We also propose a novel semantically-
12 guided self-supervision mechanism which further improves
13 the performance of the agent on unseen environments. The
14 cross-modal embeddings learned during training suggest that
15 common sense and semantic understanding helps in captur-
16 ing the structural and positional patterns of the environment,
17 implying that the agent benefits by inherently learning a map
18 of the environment.

Introduction

19
20 Most previous embodied agent research focuses on combin-
21 ing language and visual inputs (Das et al. 2017, 2018;
22 Gordon et al. 2017; Manolis Savva et al. 2019; Mirowski
23 et al. 2018; Anderson et al. 2017; Fried et al. 2018; Wang
24 et al. 2018). However, recent research suggests that using
25 language instructions alone can outperform models with vi-
26 sual features (Anand et al. 2018; Hu et al. 2019). It raises
27 the question of what the agent actually learns from both the
28 visual and language inputs, and if there is any underlying
29 features that the agent can benefit from.

30 Most past research ignores intrinsic features such as com-
31 mon sense of the environment settings and encoded scene-
32 relevant information such as semantic understanding. Thus,
33 previous agents need to rely on step-by-step instructions
34 (Shridhar et al. 2020) to navigate to the target successfully,
35 especially in a new environment. In comparison, humans do
36 not require low-level instructions such as “go straight for five
37 meters, and turn left at the end of the hallway” to navigate to
38 the restroom in a new restaurant. Instead, humans leverage
39 intrinsically embedded features such as scene information
40 and common sense of room layouts to navigate in an unseen

environment. Automated agents, however, have difficulties
41 in performing grounded language navigation tasks with ab-
42 stract, high-level instructions such as “go to the kitchen” in
43 realistic unseen 3D environments (Tangiuchi et al. 2019).
44 We hypothesize that common sense of room layout and se-
45 mantic understanding of the environment can benefit agents
46 in a similar way as they benefit humans. Specifically, com-
47 mon sense of room layout can assist path planning by setting
48 the general course of the trajectory. For instance, when nav-
49 igating to the kitchen, it is useful to know that a dining room
50 is usually close to a kitchen. On the other hand, semantic un-
51 derstanding of the room (i.e. objects in each room, etc.) sup-
52 ports better local actions. For example, agents should stop
53 when the target room is reached. 54

55 In this work, we explore the role of common sense room
56 layout and room semantic understanding in the concept-
57 driven room navigation task. Figure 1 describes an example
58 of the *RoomNav* task. An agent is spawn randomly in a re-
59 alistic 3D house environment with a given instruction (e.g.
60 “go to the restroom”). Then the agent has to navigate to
61 the target room by performing a sequence of actions: turn
62 left, turn right, move forward, or stop. This paper’s objec-
63 tive is not to build an agent which outperforms the state-
64 of-the-art in the *RoomNav* task. Instead, the primary focus
65 of our research is to explore the research question related
66 to grounded language understanding without data bias is-
67 sues seen in previous research: can intrinsic features such as
68 common sense and semantic grounded understanding of the
69 environment also help the agent navigate with high-level in-
70 structions? Our contributions to address the problem are the
71 following: (i) we proposed novel ways to incorporate com-
72 mon sense and semantic understanding within the artificial
73 agents to address a complex task in the multi-modal setting
74 inspired by humans (ii) proposed semantically-guided self-
75 supervised imitation learning (*SIL*) mechanism for ground-
76 ing to fine-tune the agent on unseen environments for gen-
77 eralization ability (iii) showed that common sense facilitates
78 long-term while semantic grounding facilitates local plan-
79 ning, and (iv) demonstrated that the reason common sense
80 and semantic grounded understanding help with navigation
81 is by mapping learned instruction embeddings to the scenes.



Figure 1: Illustration of the RoomNav task. At each timestep, the agent observes a panoramic view (left, front and right views concatenated) with dining room on the left, living room ahead, wall on the right, and hallway being current. The agent is spawned in a random location and is asked to navigate to the target room with a high-level instruction (“Go to the kitchen”) using four possible actions: turn right, turn left, go forward, and stop.

Related Work

Previous related research in embodied environments lie in comparing vision and language-grounded tasks, exploring potential underlying features of the environment, and making agents more robust towards unseen environments.

Vision and Language Grounded Tasks: Embodied question answering (Das et al. 2017) and instruction following (Anderson et al. 2017; Shridhar et al. 2020) in embodied environments have been popular to study the interaction between language and visual inputs. We choose the *RoomNav* task to test the research question that whether equipping an agent with similar high-level inputs as humans (common sense and semantic understanding) can help with downstream navigation tasks by eliminating other factors such as data bias seen in instruction following tasks (Hu et al. 2019).

Common Sense and Understanding: Some recent research explores semantic representation and common sense knowledge graph in object navigation tasks in simpler environment settings (Hermann et al. 2017). Mousavian et al. (2018) use pre-trained object detection or segmentation models to represent semantics to navigate to five semantic goals in nine homes. Yang et al. (2019) extract relationships among objects into a knowledge graph with a Graph Convolution (Kipf and Welling 2017) encoding as priors to the navigation model. Gupta et al. (2017) propose a spatial memory map by projecting environment information to a 2D matrix. Recently, Wu et al. (2019) proposed to model relational memory among room types in navigation tasks using a Bayesian probabilistic relational graph. We instead adopt a simple backward language model to model common sense. In our work, we train the agent to learn semantics and common sense together in navigation. Instead of abstracting visual and language representations, we illustrate whether providing these inputs can help with embodied tasks. In addition, we leverage the learned models and further fine-tune the agent in novel environments. We also demonstrate the causality by analyzing what the agent learns.

Robustification: Several studies have analyzed robustification and generalization to unseen environments, using methods such as reinforcement learning and semi-supervised learning. Manolis Savva et al. (2019) apply Proximal Policy Optimization (Schulman et al. 2017) for point-nav task guided by a very strong signal of the relative distance between the agent and the target coordinate. Wang et al. (2018) fine-tune the agent on unseen environments using a cycle-reconstruction loss obtained by reversing the original instruction following problem (Fried et al. 2018). For a similar *RoomNav* task, Wu et al. (2018a) use Deep Deterministic Policy Gradient (Heess et al. 2015) and Asynchronous Advantage Actor Critic (Mnih et al. 2016) on the semantically rich House3D (Wu et al. 2018b) environment. These learned policies do not leverage any intrinsic common sense and knowledge-grounded semantic information available in the environment. We perform SIL by introducing auxiliary tasks related to semantic understanding to make the model generalize to unseen environments better. Furthermore, we analyze the common sense that the agent learns from SIL and why SIL improves the performance on unseen environments by evaluating the understanding of the agent on the input instructions.

Common Sense and Semantically Grounded Agent

We first introduce the agent architecture, and then the learning process.

Agent Architecture

Our architecture consists of four components: Base Navigation, Common Sense Planning, Semantic Grounding, and Semantic-Grounded Navigator. We also explain how the agent functions can be fine-tuned on unseen environments without annotations. Figure 2 shows the entire architecture framework and Figure 6 in the Appendix depicts detailed architecture with model information along with loss functions.

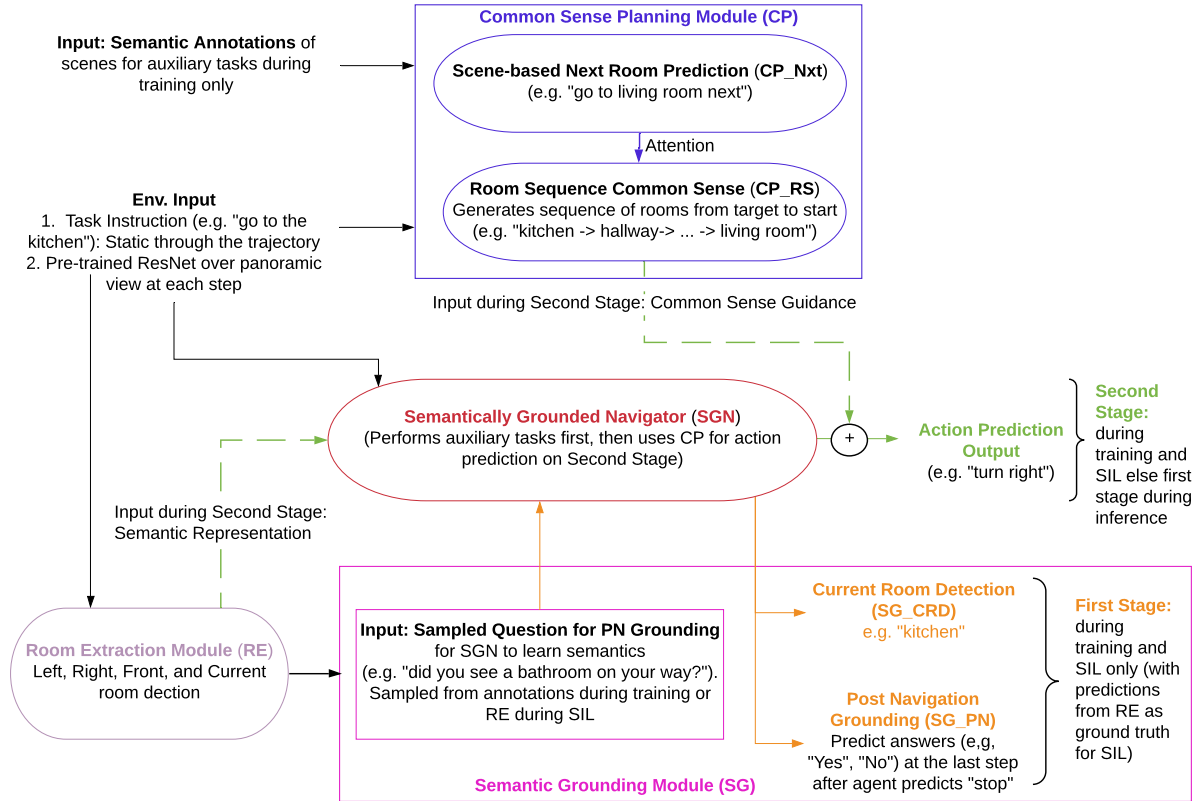


Figure 2: High-level architecture of Common Sense and Semantically Grounded Navigation model. Red components correspond to Base Navigation model. Purple components are introduced to incorporate common sense while pink components are used for semantic understanding. The Semantically Grounded Navigator (SGN) is designed to perform semantic understanding for action prediction, while common sense is fed as guidance for better planning. Dotted lines indicate input in the second pass in the model. A detailed architecture with model information and illustration with all the loss functions can be found in Figure 6 in the Appendix.

155 **Base Navigation** We use an LSTM-based (Hochreiter and
 156 Schmidhuber 1997) navigation model following the work in
 157 Das et al. (2017) to train a navigation agent which predicts
 158 an action given the current state. The input to the LSTM is
 159 the context of the path, *RoomNav* instructions (e.g. “go to
 160 the kitchen”), a visual representation of the scene, and the
 161 previous action following Das et al. (2017). We choose the
 162 simple LSTM baseline as opposed to a state-of-the-art nav-
 163 igation model because the components we introduce are or-
 164 thogonal to the previous contributions which did not utilize
 165 this available information from the environment. In addition,
 166 using a simple model reduces the influence from interacting
 167 with different complex modules, and thus disentangles the
 168 contribution of incorporating common sense and semantic
 169 understanding.

170 **Common Sense Planning Module (CP)** We hypothesize
 171 that realistic house environments follow common sense such
 172 as structural patterns (e.g. a refrigerator is usually placed in
 173 the kitchen) and sequential patterns (e.g. a kitchen is usually
 174 near a dining room). To incorporate such common sense in-

formation in the agent, we design two auxiliary tasks in the
 175 *CP* module: Scene-based Next Room Prediction (*CP_Nxt*)
 176 and Room Sequence Common Sense (*CP_RS*) using room
 177 sequences observed from training environments. *CP_Nxt*
 178 module enables the agent to predict and navigate to inter-
 179 mediate targets to deal with the fact that the target room in the
 180 instruction may be distant and thus hard to interpret. Specif-
 181 ically, we train the agent to predict the next room as an in-
 182 termediate goal at every time step. For instance, in Figure
 183 1, the agent is in the hallway, and the *CP_Nxt* module will
 184 predict the next room to move to as “dining room”, since it
 185 is the closest room on the potential path to the target location
 186 (the kitchen).
 187

The *CP_Nxt* module is hinted by the current scene and
 188 the target room from the instruction, but it does not take into
 189 account what rooms are connected to the target room. To
 190 rectify such misalignment, we design *CP_RS* to generate
 191 backward room sequences that start from the target room
 192 using an LSTM model, similar to an auto-regressive lan-
 193 guage model. We then obtain a contextual representation by
 194 attending *CP_Nxt* hidden state to each state representation
 195

196 in the output of the *CP_RS* module before predicting the
197 next room accordingly.

198 **Semantic Grounding Module (*SG*)** We design two sub-
199 modules in *SG* to help the agent to understand the semantics
200 of the environment: (i) Current Room Detection (*SG_CRD*)
201 for detecting the current room at each timestep to capture lo-
202 cal semantics and (ii) Post Navigation Grounding (*SG_PN*)
203 for understanding and capturing the global semantics along
204 the trajectory. We cast *SG_CRD* as a multi-label classifica-
205 tion problem to detect the room type on top of the hidden
206 states from the base navigation LSTM. In comparison, we
207 cast the *SG_PN* as a binary classification problem to pre-
208 dict if there is a certain room type on the trajectory using the
209 last hidden state with a sampled question (e.g. “did you see
210 a bathroom on the way”) from the environment annotations.

211 **Semantic-grounded Navigator (*SGN*)** *SGN* incorpo-
212 rates *CP* and *SG* into the Base Navigation model. Our
213 *SGN* first adopts the LSTM baseline model and generates
214 a state at every step that is used in multiple tasks: (i) ac-
215 tion prediction to perform one of the four possible actions
216 at each step: go forward (0.25m), turn left (10 degrees), turn
217 right (10 degrees), and stop; (ii) semantic grounding via cur-
218 rent room detection (*SG_CRD*); and (iii) semantic grounding
219 via post-navigation grounding (*SG_PN*). The *SGN* takes the
220 *RoomNav* instruction (which is fixed throughout the task)
221 and the visual representation (which changes at each step)
222 as input. In specific, *SGN* predicts the current room for
223 *SG_CRD* using a linear layer on top of each *SGN* hidden
224 state and predicts post-navigation answer on the last *SGN*
225 hidden state. For action prediction at each timestep, the *SGN*
226 hidden state attends to each hidden state of the generic room
227 sequence in *CP_RS* to obtain a contextual representation.
228 The attention-based representation is then concatenated with
229 the original *SGN* hidden state to predict the next action.
230 Please refer to Figure 6 in the Appendix for more details.

231 **Two-stage *SGN* for Self-supervised Learning with Room**
232 **Extraction (*RE*) Module** In an unseen environment, we
233 aim to build an agent which can update its action predic-
234 tion by aligning what it has learned already to the unique
235 patterns and semantics observed in the new setting. Humans
236 are capable of doing this because they have semantic under-
237 standing: humans fine-tune their action prediction in an un-
238 seen environment according to newer semantic observations.
239 Since there is no semantic annotation for unseen environ-
240 ments, we need to simulate the annotations as ground-truth
241 to fine-tune the *SGN* module in a self-supervised setting. To
242 get extra pseudo labels, we introduce the Room Extraction
243 Module (*RE*).

244 The *RE* module detects the current room and the rooms
245 on the left, right, and front given the panoramic represen-
246 tation, which facilitates the agent to understand semantics
247 from different angles. We implement the *RE* module with
248 a multi-layer perceptron (MLP) on the image representa-
249 tion and add different heads for different room extraction.
250 Note that the major difference between *RE* and *SG_CRD*
251 is the input to the modules: *RE* takes image features in-
252 dependently from the agent while *SG_CRD* takes hidden

states from *SGN* as input for room detection. Specifically, 253
RE is a separate model to extract semantics, agnostic to 254
instructions and trajectories. In comparison, *SG_CRD* en- 255
codes the instruction and the trajectory history. More impor- 256
tantly, *SG_CRD* shares parameters with *SGN* which pre- 257
dicts actions. Therefore, we take *RE* predictions as pseudo 258
ground-truth and fine-tune *SG_CRD* on top of *SGN* so that 259
we can achieve the goal of fine-tuning action prediction. 260

261 Because we need independent features to predict the same 261
objective from *RE* and *SG_CRD*, we design a two-stage 262
training process over the *SGN* at each time step to per- 263
form grounding along with navigation. In the first stage, the 264
Current Room Detection task (*SG_CRD*) on top of *SGN* 265
is performed without information flowing from *RE* repre- 266
sentations by masking. The reason for masking *RE* repre- 267
sentation is that *RE* hidden states are optimized for room 268
extractions in different angles with its training objective, 269
which already contains room detection features. Without 270
RE hidden state, *SGN* is encouraged to capture seman- 271
tics for *SGN_CRD* to detect room information independ- 272
ently using raw scene information and previous *SGN* hid- 273
den states. On the other hand, if *RE* outputs are considered 274
as features, *SG_CRD* may simply copy the representations 275
without utilizing the learned semantics. Similarly, Post Nav- 276
igation Grounding task (*SG_PN*) on top of *SGN* is per- 277
formed only at the last state when “stop” action is received 278
in the first stage. In the second stage, we feed output repre- 279
sentations from *CP* and *RE* modules (depicted via dotted 280
lines in Figure 2) into *SGN* to perform action prediction. 281
The reason to incorporate *RE* representation, which extracts 282
features directly from image input, is that abstracted seman- 283
tics are shown to help with navigation as seen in previous re- 284
search (Mousavian et al. 2018; Hudson and Manning 2019). 285

286 With the two-stage training objectives, we can perform 286
self-supervised learning (SIL) on unseen environments to 287
update the agent for better semantic understanding. In spe- 288
cific, we take the prediction from *RE* as ground truth labels 289
and fine-tune the *SG_CRD* and *SG_PN* heads together 290
with the *SGN* for action prediction. The agent explores the 291
environment according to the trained *SGN* for a pre-defined 292
 t steps to get familiarized with the new environment, cal- 293
culates losses between the two room detection models, and 294
finally updates the parameters for the LSTM in *SGN*. The 295
agent then navigates towards the target room from the start- 296
ing location using the fine-tuned parameters. 297

298 Learning Procedure

299 We train the agent in two ways: (i) imitation learning (*IL*) 299
with shortest path trajectories available during training, and 300
(ii) self-supervised imitation learning (*SIL*) on unseen en- 301
vironments, inspired by the work from (Wang et al. 2018). 302
During *IL*, apart from the main action prediction task, 303
we perform five auxiliary tasks: 1. next room detection 304
(*CP_Nxt*) 2. target to source room sequence prediction 305
(*CP_RS*) 3. current and surrounding rooms extraction (*RE*) 306
4. post navigation response generation (*SG_PN*) and 5. cur- 307
rent room predictions on top of *SGN* for the first stage 308
(*SG_CRD*). In total, we have six losses during imitation 309
learning including action prediction. The overall loss func- 310

Module	succ. rate	easy succ. rate	med. succ. rate	hard succ. rate
Baseline	0.25	0.41	0.24	0.17
+ Common Sense (CS)	0.30	0.44	0.29	0.25
+ Semantic Grounding (SG)	0.28	0.53	0.24	0.19
+ SG + SIL	0.36	0.56	0.40	0.21
+ CP + SG + SIL	0.39	0.56	0.40	0.28

Table 1: Results on Imitation Learning (IL) and Self-supervised IL (SIL) for easy, medium, and hard trajectories on unseen test environments. For Common Sense Planning (CP), CP_Nxt represents next room prediction while CP_RS utilizes room sequence. For Semantic Ground (SG), room extraction (RE) identifies current and nearby rooms on input images, while SG_CRD and SG_PN performs current room detection at each timestep for local semantics and post navigation for global semantics, respectively, on hidden states.

tion is:

$$L_{IL} = \lambda_a * L_{action} + \lambda_{CP_Nxt} * L_{CP_Nxt} + \lambda_{CP_RS} * L_{CP_RS} + \lambda_{RE} * L_{RE} + \lambda_{SG_PN} * L_{SG_PN} + \lambda_{SGN_CRD} * L_{SGN_CRD} \quad (1)$$

where the loss for each task is the cross-entropy loss between the prediction and the annotations in the environment on either the last state (for SG_PN only) or for each state in the SGN (for other modules).

For SIL on unseen environments, we obtain losses from SG_CRD using RE predictions as target labels at each time step and from SG_PN at the end of the exploration. The loss function is represented as:

$$L_{SIL} = \lambda_{SG_CRD} * L'_{SG_CRD} + \lambda_{SG_PN} * L'_{SG_PN} \quad (2)$$

where L'_{SG_CRD} and L'_{SG_PN} indicates the loss using simulated labels on unseen environments, in comparison with L_{SG_CRD} and L_{SG_PN} using true ground-truth labels on annotated training environments.

Experiments

Data and Environment: We use Habitat Simulator and corresponding APIs (Manolis Savva et al. 2019) to render the MatterPort3D environment for all our tasks. One of the key tasks in MatterPort3D dataset is point navigation, wherein an agent needs to navigate from a source coordinate to a target coordinate. We adapt this task to form a *RoomNav* task by replacing the target coordinates with the corresponding 27 room types annotated in the dataset (excluding “other room”). We remove those trajectories where the target and the source rooms are the same and the ones where the target is at the border of several rooms. There are in total 53 houses and 5020 trajectories in training, 11 houses and 168 trajectories for validation, and 15 houses and 324 trajectories for testing. To measure the complexity of each trajectory, we use the same measure as the point navigation task, which is the ratio of geodisic distance to that of the euclidean distance, where higher ratio indicates harder tasks. The average number of rooms between the source and target is 2.41, 3.01, and

4.06, in easy, medium, and hard trajectories in the training data respectively.

Model Input: The SGN has two types of input: (i) Environment input including task specific instruction (e.g. “go to the kitchen”) and RGB values of visual observations in each state, and (ii) semantic information such as room annotations for training RE and sampled questions for PN . Semantic information is used in semantic predictions and question generation during training only, because such information is not available on unseen environments. Following previous embodied navigation work (Fried et al. 2018; Wang et al. 2018), we extract panoramic image features using a fixed pretrained ResNet-152 (He et al. 2015). Specifically, we turn the agent 90 degrees to the left and right to obtain a 270-degree view at each timestep. We extract and concatenate features in the left, front, and right images and then pass through a single feed forward layer to obtain the environment visual representation. In order to evaluate the information gained from semantic understanding instead of memorizing segments or detecting obstructions, we only use RGB features in our model instead of features from other sensors, such as semantic masking features (Wu et al. 2018a) or depth features.

Hyperparameter tuning: We use the validation set to tune the hyperparameters including the weights in each of the tasks in equation 1. In specific, we set the weight of action prediction loss to 1 and do grid search for other weights.

Evaluation Metrics: We use three evaluation metrics: success rate, success per length (SPL) following Wang et al. (2018), and non-stop SPL. Success rate is defined as the percentage of trajectories where the agent enters the target room. Success per length (SPL) is defined as the success rate normalized by the shortest path. In particular, SPL considers a game successful only if the agent predicts the “stop” action inside the target room, which is infrequently seen (about once every 71 steps) compared to other actions during training. We use *non-stop SPL* to relax this constraint to count the percentage of trajectories in which agent enters the target room during the trajectory. We note that non-stop SPL is a relatively weak metric, but we include this less sensitive metric against the “stop” action to indicate how well the agent can navigate to the target room. In other words, non-stop SPL can indicate the agent’s performance on path

386 planning. We also report average steps, which directly de- 441
387 termines SPL, to indicate the number of steps the agent ex- 442
388 plores before predicting “stop” (with the maximum number 443
389 of steps set to 200, and the average number of steps in the 444
390 annotated trajectories for training is 82). 445

391 Results 446

392 We first analyze results for imitation learning and self- 447
393 supervised imitation learning. Then we interpret why the 448
394 agent benefits from the proposed model by interpreting the 449
395 learned embedding alignments. 450

396 Imitation learning 451

397 We observe in Table 1 that common sense planning and se- 452
398 mantic understanding help in the imitation learning setting 453
399 across the board when compared to the *LSTM* baseline 454
400 model that does not incorporate these modules. Note that 455
401 common sense and semantic information is not fed as fea- 456
402 tures to the agent, rather is learnt via auxiliary tasks. 457

403 **Common Sense Planning:** We incorporate common 458
404 sense via two sub-tasks: (i) next room guidance (*CP_Nxt*) 459
405 and (ii) generic room sequence from target to source room 460
406 (*CP_RS*) as described in section . Results show that *CP* mod- 461
407 ules improve navigation performances in medium and harder 462
408 trajectories more than the easy trajectories and hence in- 463
409 dicates that they help with long-term planning. Next room 464
410 prediction alone leads to significant improvement in *SPL* 465
411 (80% improvement over the baseline) and the second best 466
412 success rate in hard tasks (40% improvement over baseline). 467
413 When we combine with room sequence module, the agent’s 468
414 performance improves in both easy and medium trajecto- 469
415 ries, but not in hard trajectories. This suggests that room se- 470
416 quence module learns generic patterns, but for hard trajecto- 471
417 ries where geodesic distance is significantly higher than the 472
418 euclidean distance, *CP_RS* does not help much probably 473
419 due to incorrect long sequence predictions. 474

420 **Semantic Understanding** is incorporated via three dif- 475
421 ferent tasks: (i) a separate room identification model which 476
422 predicts nearby rooms (*RE*) given current views using the 477
423 shared *ResNet* input. (ii) current room prediction given 478
424 the *SGN* hidden state (*SGN_CRD*) (iii) post-navigation 479
425 grounding with sampled question (*SGN_PN*). Results sug- 480
426 gest that incorporating semantic understanding generally 481
427 improves short-term planning compared to an agent with- 482
428 out semantic understanding (baseline). It is observed that the 483
429 agent fed with *RE* and *SG_CRD* tends to achieve higher 484
430 *SPL* scores because it usually stops early with less aver- 485
431 age number of steps to complete the task. At the same time, 486
432 the early stopping can also explain the low performances on 487
433 medium and hard trajectories. *SG_PN* does not follow a sim- 488
434 ilar pattern because grounding in this case is performed at 489
435 the terminal state, hence it does not impact turn-level action 490
436 prediction directly, leading to longer trajectories. Moreover, 491
437 *SG_PN* does better on medium and hard trajectories be- 492
438 cause it lets the navigator (*SGN*) focus more on intermediate 493
439 action predictions while ensuring semantic understanding at 494
440 the terminal state. 495

441 Combing the two room detection objectives together 442
443 (*RE+SG_CRD*), we get the second best *SPL* score (0.141, 444
445 110% better than the baseline) but improvements are mostly 446
447 on easy trajectories. This indicates that the agent might tend 448
449 to focus more on the auxiliary task than on the original ac- 449
450 tion prediction task. However, adding *SG_PN* to step level 450
451 *RE* and *SG_CRD* modules to facilitate semantic under- 451
452 standing from a global perspective leads to significant in- 452
453 crease in performance for medium and hard trajectories, 453
454 while maintaining high *SPL* scores. 454

455 **Discussion:** Note that the average number of steps is 455
456 higher than that in the annotated trajectory (82). From our 456
457 qualitative analysis by evaluating the generated videos along 457
458 the testing trajectories, the main reason for higher average 458
459 steps is that the agent can get stuck in front of an object such 459
460 as a table (by predicting turning and going forward consis- 460
461 tently). This indicates that the agent does not achieve the 461
462 goal by chance roaming around the environment. In addi- 462
463 tion, different performances in different metrics such as suc- 463
464 cess rate in multiple difficulty levels suggest that our pro- 464
465 posed modules are complementary to each other since they 465
466 are helping navigation in different perspectives. 466

467 Self-supervised Imitation Learning 468

469 To perform *SIL*, we either use current room prediction 469
470 (*SG_CRD*) or post navigation grounding (*SG_PN*) or both 470
471 as the auxiliary task to fine-tune the Semantically Grounded 471
472 Navigator (*SGN*) to get a loss function against the simulated 472
473 target label using *RE*. While performing *SIL*, we found 473
474 that by letting the agent explore unseen environments for 20 474
475 steps ($t = 20$) before actually executing the instruction and 475
476 navigating to the target significantly improves the perfor- 476
477 mance (7% with *RE + SG_CRD*, 22% with *RE + SG_PN* and 477
478 *RE + SG_CRD + SG_PN*). Similar to the pattern observed 478
479 without *SIL*, using local semantic grounding (*SG_CRD*) 479
480 performs better on easier trajectories while using global se- 480
481 mantic grounding by post-navigation questions (*SG_PN*) 481
482 achieves better performance on harder trajectories. Finally, 482
483 when we combine all the proposed *CP* and *SG* modules and 483
484 perform *SIL*, we get the best performance overall with 56% 484
485 improvement over non-stop *SPL* and 64% improvement over 485
486 *SPL*, with maximum improvements on medium and hard 486
487 trajectories. Note that the low absolute scores on *SPL* and 487
488 non-stop *SPL* indicates that room navigation with low-level 488
489 instructions on unseen environment for generalization is a 489
490 hard task. We also observe that when we further fine-tune the 490
491 agent in the *SIL* setting with more steps (with $t = 40, 60$), 491
492 the performance degrades drastically as the model tends to 492
493 overfit to noises of the approximate pseudo labels obtained 493
494 from the *RE* model. 494

495 Cross-modal Embeddings 496

497 To identify why *CP* and semantic understanding helps in the 497
498 navigation task, we analyzed the cross-modal embeddings 498
499 learnt during training to show how the agent interpret lan- 499
500 guage instructions. Traditional embeddings such as GloVe 500
501 (Pennington, Socher, and Manning 2014), are functions of 501
502 words or semantic entities appearing in similar contexts and 502

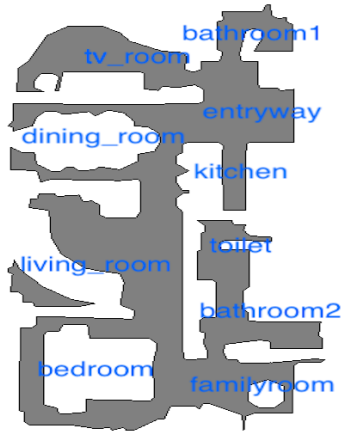


Figure 3: Top view of a house layout with dark areas as obstacles

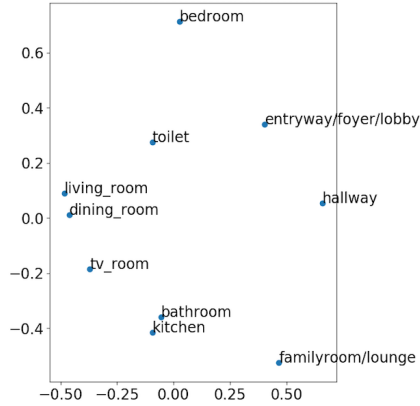


Figure 4: Embeddings of *RE + SG_CRD* model trained on all the training environments mapped to 2D space with PCA

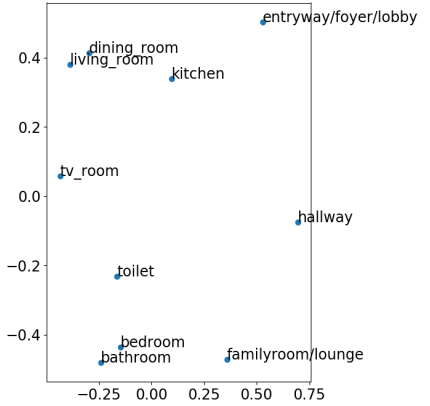


Figure 5: Embeddings of *RE + SG_CRD* model after SIL fine-tuning on the environment in Figure 3 mapped to 2D space.

497 may not capture the visual and structural properties of entities in realistic 3D worlds. Therefore, we first randomly
 498 initialize the cross-modal embeddings and then train them
 499 with the proposed modules across multiple trajectories in
 500 different environments. We qualitatively analyze these embeddings
 501 to explore if they reflect any structural or visual characteristics
 502 of the environment. Figure 3 represents the top-view of an environment
 503 and Figure 4 visualizes the embeddings trained using the *RE + SG_CRD*
 504 model by dimension reduction using PCA (while other models illustrate
 505 similar patterns). The figure shows that the learned embeddings
 506 capture the average structural pattern of rooms across all the
 507 environments. We further fine-tune the agent and the embeddings
 508 on the example environment shown in Figure 3 using self-supervised
 509 imitation learning and visualize it in Figure 5. We observe that the
 510 fine-tuned embeddings tend to mimic the structural and positional
 511 patterns of the exact environment. This indicates that the proposed
 512 models help the agent to understand the instructions better by aligning
 513 the instruction encoding with the actual scene information. We
 514 conjecture that such alignment, which is learned from the proposed
 515 common sense and semantic grounding modules, explains what the
 516 model actually learns. The close mapping between the fine-tuned
 517 word embeddings of the room types and the structure of the environment
 518 draws connections to the SLAM (Durrant-Whyte and Bailey 2006)
 519 algorithm, which is one of the most popular mapping algorithms
 520 for navigation. However, we can leverage what the agent has
 521 already learned as a prior instead of exhaustively exploring each
 522 room for SLAM. This alignment also draws connection to recent
 523 research on vision-and-language pre-training such as VisualBERT
 524 (Li et al. 2019) which is optimized to align text and image regions
 525 with self-attention. We leave the detailed comparison to future work.

Conclusion

531 Humans navigate to rooms on unseen environments leveraging
 532 common sense of room layout and semantic understanding of the
 533 environment. We propose to simulate human navigation by
 534 incorporating these features ignored in previous research. The
 535 goal of this paper is not to build a state-of-the-art navigation
 536 system, but using the navigation environment to explore if
 537 common sense and semantic grounding is useful in visual navigation.
 538 We introduced methods to incorporate these features and showed
 539 that common sense and semantic grounding help in long-term
 540 and short-term planning respectively for effective navigation.
 541 We also found out that the agent fine-tuned using self-supervised
 542 imitation learning generalizes better to unseen environments.
 543 Furthermore, we analyzed the reason for such improvement by
 544 inspecting cross-modal embeddings obtained during training,
 545 which captures structural and positional patterns of the environment.
 546 This suggests that the agent learns a semantic map of the environment
 547 in the process of the navigation.

References

- 551 Anand, A.; Belilovsky, E.; Kastner, K.; Larochelle, H.; and
 552 Courville, A. C. 2018. Blindfold Baselines for Embodied
 553 QA. *CoRR* abs/1811.05013. URL <http://arxiv.org/abs/1811.05013>.
 554
- 555 Anderson, P.; Wu, Q.; Teney, D.; Bruce, J.; Johnson, M.;
 556 Sünderhauf, N.; Reid, I. D.; Gould, S.; and van den Hengel,
 557 A. 2017. Vision-and-Language Navigation: Interpreting
 558 visually-grounded navigation instructions in real environments.
 559 *CoRR* abs/1711.07280. URL <http://arxiv.org/abs/1711.07280>.
 560
- 561 Das, A.; Datta, S.; Gkioxari, G.; Lee, S.; Parikh, D.; and
 562 Batra, D. 2017. Embodied Question Answering. *CoRR*
 563 abs/1711.11543. URL <http://arxiv.org/abs/1711.11543>.
 564
- 565 Das, A.; Gkioxari, G.; Lee, S.; Parikh, D.; and Batra, D.
 2018. Neural Modular Control for Embodied Question An-

566 swering. *CoRR* abs/1810.11181. URL <http://arxiv.org/abs/1810.11181>. 619

567 1810.11181. 620

568 Durrant-Whyte, H. F.; and Bailey, T. 2006. Simultaneous lo- 621

569 calization and mapping: part I. *IEEE Robot. Automat. Mag.* 622

570 13(2): 99–110. doi:10.1109/MRA.2006.1638022. URL 623

571 <https://doi.org/10.1109/MRA.2006.1638022>. 624

572 Fried, D.; Hu, R.; Cirik, V.; Rohrbach, A.; Andreas, J.; 625

573 Morency, L.; Berg-Kirkpatrick, T.; Saenko, K.; Klein, D.; 626

574 and Darrell, T. 2018. Speaker-Follower Models for Vision- 627

575 and-Language Navigation. *CoRR* abs/1806.02724. URL 628

576 <http://arxiv.org/abs/1806.02724>. 629

577 Gordon, D.; Kembhavi, A.; Rastegari, M.; Redmon, J.; Fox, 630

578 D.; and Farhadi, A. 2017. IQA: Visual Question Answering 631

579 in Interactive Environments. *CoRR* abs/1712.03316. URL 632

580 <http://arxiv.org/abs/1712.03316>. 633

581 Gupta, S.; Davidson, J.; Levine, S.; Sukthankar, R.; and Ma- 634

582 lik, J. 2017. Cognitive Mapping and Planning for Visual 635

583 Navigation. *CoRR* abs/1702.03920. URL <http://arxiv.org/abs/1702.03920>. 636

584 637

585 He, K.; Zhang, X.; Ren, S.; and Sun, J. 2015. Deep Resid- 638

586 ual Learning for Image Recognition. *CoRR* abs/1512.03385. 639

587 URL <http://arxiv.org/abs/1512.03385>. 640

588 Heess, N.; Wayne, G.; Silver, D.; Lillicrap, T. P.; Tassa, Y.; 641

589 and Erez, T. 2015. Learning Continuous Control Policies by 642

590 Stochastic Value Gradients. *CoRR* abs/1510.09142. URL 643

591 <http://arxiv.org/abs/1510.09142>. 644

592 Hermann, K. M.; Hill, F.; Green, S.; Wang, F.; Faulkner, 645

593 R.; Soyer, H.; Szepesvari, D.; Czarnecki, W. M.; Jaderberg, 646

594 M.; Teplyashin, D.; Wainwright, M.; Apps, C.; Hassabis, 647

595 D.; and Blunsom, P. 2017. Grounded Language Learning 648

596 in a Simulated 3D World. *CoRR* abs/1706.06551. URL 649

597 <http://arxiv.org/abs/1706.06551>. 650

598 Hochreiter, S.; and Schmidhuber, J. 1997. Long short-term 651

599 memory. *Neural computation* 9(8): 1735–1780. 652

600 Hu, R.; Fried, D.; Rohrbach, A.; Klein, D.; Darrell, T.; and 653

601 Saenko, K. 2019. Are You Looking? Grounding to Multi- 654

602 ple Modalities in Vision-and-Language Navigation. *CoRR* 655

603 abs/1906.00347. URL <http://arxiv.org/abs/1906.00347>. 656

604 Hudson, D. A.; and Manning, C. D. 2019. Learning by Ab- 657

605 straction: The Neural State Machine. *CoRR* abs/1907.03950. 658

606 URL <http://arxiv.org/abs/1907.03950>. 659

607 Kipf, T. N.; and Welling, M. 2017. Semi-Supervised Clas- 660

608 sification with Graph Convolutional Networks. In *Internat-* 661

609 *ional Conference on Learning Representations (ICLR)*. 662

610 Li, L. H.; Yatskar, M.; Yin, D.; Hsieh, C.-J.; and Chang, K.- 663

611 W. 2019. VisualBERT: A Simple and Performant Baseline 664

612 for Vision and Language. 665

613 Manolis Savva; Abhishek Kadian; Oleksandr Maksymets; 666

614 Zhao, Y.; Wijmans, E.; Jain, B.; Straub, J.; Liu, J.; Koltun, 667

615 V.; Malik, J.; Parikh, D.; and Batra, D. 2019. Habitat: A 668

616 Platform for Embodied AI Research. In *Proceedings of* 669

617 *the IEEE/CVF International Conference on Computer Vi-* 670

618 *sion (ICCV)*. 671

Mirowski, P.; Grimes, M. K.; Malinowski, M.; Hermann, 672

K. M.; Anderson, K.; Teplyashin, D.; Simonyan, K.; 673

Kavukcuoglu, K.; Zisserman, A.; and Hadsell, R. 2018. 674

Learning to Navigate in Cities Without a Map. *CoRR* 675

abs/1804.00168. URL <http://arxiv.org/abs/1804.00168>. 676

Mnih, V.; Badia, A. P.; Mirza, M.; Graves, A.; Lillicrap, 677

T. P.; Harley, T.; Silver, D.; and Kavukcuoglu, K. 2016. 678

Asynchronous Methods for Deep Reinforcement Learn- 679

ing. *CoRR* abs/1602.01783. URL <http://arxiv.org/abs/1602.01783>. 680

Mousavian, A.; Toshev, A.; Fiser, M.; Kosecka, J.; and 681

Davidson, J. 2018. Visual Representations for Semantic 682

Target Driven Navigation. *CoRR* abs/1805.06066. URL 683

<http://arxiv.org/abs/1805.06066>. 684

Pennington, J.; Socher, R.; and Manning, C. D. 2014. Glove: 685

Global Vectors for Word Representation. In *Proceedings* 686

of the 2014 Conference on Empirical Methods in Natu- 687

ral Language Processing, EMNLP 2014, October 25-29, 688

2014, Doha, Qatar, A meeting of SIGDAT, a Special Interest 689

Group of the ACL, 1532–1543. URL <https://www.aclweb.org/anthology/D14-1162/>. 690

Schulman, J.; Wolski, F.; Dhariwal, P.; Radford, A.; and 691

Klimov, O. 2017. Proximal Policy Optimization Algo- 692

rithms. *CoRR* abs/1707.06347. URL <http://arxiv.org/abs/1707.06347>. 693

Shridhar, M.; Thomason, J.; Gordon, D.; Bisk, Y.; Han, 694

W.; Mottaghi, R.; Zettlemoyer, L.; and Fox, D. 2020. AL- 695

FRED: A Benchmark for Interpreting Grounded Instruc- 696

tions for Everyday Tasks. In *The IEEE Conference on* 697

Computer Vision and Pattern Recognition (CVPR). URL 698

<https://arxiv.org/abs/1912.01734>. 699

Tangiuchi, T.; Mochihashi, D.; Nagai, T.; Uchida, S.; In- 700

oue, N.; Kobayashi, I.; Nakamura, T.; Hagiwara, Y.; Iwa- 701

hashi, N.; and Inamura, T. 2019. Survey on frontiers of 702

language and robotics. *Advanced Robotics* 1–31. doi: 703

10.1080/01691864.2019.1632223. 704

Wang, X.; Huang, Q.; Çelikyilmaz, A.; Gao, J.; Shen, 705

D.; Wang, Y.; Wang, W. Y.; and Zhang, L. 2018. Re- 706

inforced Cross-Modal Matching and Self-Supervised Im- 707

itation Learning for Vision-Language Navigation. *CoRR* 708

abs/1811.10092. URL <http://arxiv.org/abs/1811.10092>. 709

Wu, Y.; Wu, Y.; Gkioxari, G.; and Tian, Y. 2018a. Building 710

generalizable agents with a realistic and rich 3D environ- 711

ment. *arXiv preprint arXiv:1801.02209*. 712

Wu, Y.; Wu, Y.; Gkioxari, G.; and Tian, Y. 2018b. House3D: 713

A Rich and Realistic 3D Environment. *arXiv preprint* 714

arXiv:1801.02209. 715

Wu, Y.; Wu, Y.; Tamar, A.; Russell, S.; Gkioxari, G.; and 716

Tian, Y. 2019. Bayesian Relational Memory for Semantic 717

Visual Navigation. 718

Yang, W.; Wang, X.; Farhadi, A.; Gupta, A.; and Mottaghi, 719

R. 2019. Visual Semantic Navigation using Scene Priors. In 720

7th International Conference on Learning Representations, 721

ICLR 2019, New Orleans, LA, USA, May 6-9, 2019. URL 722

<https://openreview.net/forum?id=HJeRkh05Km>. 723

Appendix

